Mon. Not. R. Astron. Soc. **341,** 927–936 (2003)

Transient chaos and resonant phase mixing in violent relaxation

Henry E. Kandrup,[1,2,3★] Ileana M. Vass[1★] and Ioannis V. Sideris[1,4★]

[1]*Department of Astronomy, University of Florida, Gainesville, FL 32611, USA*
[2]*Department of Physics, University of Florida, Gainesville, FL 32611, USA*
[3]*Institute for Fundamental Theory, University of Florida, Gainesville, FL 32611, USA*
[4]*Department of Physics, Northern Illinois University, De Kalb, IL 60115, USA*

Accepted 2003 January 28. Received 2003 January 23; in original form 2002 November 6

ABSTRACT

This paper explores how orbits in a galactic potential can be impacted by large-amplitude time-dependences of the form that one might associate with galaxy or halo formation or strong encounters between pairs of galaxies. A period of time-dependence with a strong, possibly damped, oscillatory component can give rise to large amounts of *transient chaos*, and it is argued that chaotic phase mixing associated with this transient chaos could play a major role in accounting for the speed and efficiency of violent relaxation. Analysis of simple toy models involving time-dependent perturbations of an integrable Plummer potential indicates that this chaos results from a broad, possibly generic, resonance between the frequencies of the orbits and harmonics thereof and the frequencies of the time-dependent perturbation. Numerical computations of orbits in potentials exhibiting damped oscillations suggest that, within a period of 10 dynamical times $t_{\rm D}$ or so, one could achieve simultaneously both 'near-complete' chaotic phase mixing and a nearly time-independent, integrable end state.

Key words: galaxies: formation – galaxies: kinematics and dynamics.

1 MOTIVATION

Dating back at least to the pioneering work of Lynden-Bell (1967), it has been recognized that violent relaxation, viewed broadly as the mechanism whereby, even in the absence of dissipation, a galaxy evolves towards an equilibrium or near-equilibrium state, must be a collective process somehow involving phase mixing. However, not just any phase mixing will do: the simplest time-independent models that one might envision, such as Lynden-Bell's balls rolling in a pig-trough, do not approach an equilibrium nearly fast enough (cf. Kandrup 2001). For this reason, it has often been assumed that the fact that the potential is strongly time-dependent is crucial in making the mixing sufficiently efficient.

In the mid-1990s, however, it was recognized that it may not be time-dependence per se that is crucial. Rather, what seems essential is that the flow should be chaotic, exhibiting an exponentially sensitive dependence on initial conditions. The important point here (cf. Kandrup & Mahon 1994; Mahon et al. 1995; Merritt & Valluri 1996) is that, whereas the phase mixing of regular orbits proceeds as a modest power law in time, the phase mixing of chaotic orbits proceeds exponentially. Thus, for example, a localized ensemble of initial conditions corresponding to chaotic orbits will, when evolved in a time-independent Hamiltonian, begin by diverging exponentially from its localized state and then converge exponentially towards an equilibrium or near-equilibrium state (Kandrup 1998).

Unfortunately, however, most work on chaotic phase mixing hitherto has focused on flows in time-independent Hamiltonian systems, possibly allowing for low-amplitude perturbations (cf. Kandrup, Pogorelov & Sideris 2000), but ignoring the possibility of a large-amplitude time-dependence. This work on (nearly) time-independent systems confirms that chaotic phase mixing can be very efficient. However, it is clear that this phenomenon can be important only if the potential admits large measures of chaotic orbits. The obvious point, then, is that time-independent density distributions corresponding to galactic equilibria or near-equilibria are not likely to contain huge measures of chaos. As stressed, for example, by Binney (1978), interestingly shaped equilibria that might be expected to admit global stochasticity must contain large measures of regular orbits to serve as the 'skeleton' of the interesting structure.

The obvious questions, then are: might one expect to have much larger measures of chaos in realistic time-dependent systems? Should these orbits exhibit the qualitative behaviour that one would expect to observe during an epoch of violent relaxation? The aim of this paper is to argue that the answers to these questions is yes!

The crucially important point is that allowing for a time-dependent Hamiltonian can lead to resonances that trigger an epoch of *transient chaos*: even if the initial and final density distributions are nearly integrable and admit no global stochasticity, the intervening states could still correspond to orbits exhibiting significant exponential sensitivity.

★E-mail: kandrup@astro.ufl.edu (HEK); vass@astro.ufl.edu (IMV); sideris@nicadd.niu.edu (IVS)

As a paradigmatic example, one can consider a test particle moving in a spherically symmetric, constant density mass distribution that is, in addition, subjected to a periodic sinusoidal perturbation corresponding to a force per unit mass $\boldsymbol{F} = -\beta \boldsymbol{r} \cos \omega t$. In the absence of the perturbation, a particle will feel an isotropic harmonic oscillator potential and, as such, the separation $\delta \boldsymbol{r}$ between two nearby orbits will execute simple harmonic motion. However, the presence of the periodic driving complicates matters, leading to a more complex equation for $\delta \boldsymbol{r}$, a typical component of which will satisfy

$$\frac{\mathrm{d}^2 \delta r}{\mathrm{d}t^2} + \Omega^2 \delta r = 0, \qquad \text{with} \quad \Omega^2 = \alpha + \beta \cos \omega t, \tag{1}$$

a classic example of a Hill equation. The obvious point, then, is that even if α is positive and $|\beta| < \alpha$, δr can grow exponentially in time, corresponding to a chaotic orbit. The periodic driving has triggered a parametric instability.

Real systems are not of constant density, so that the unperturbed (time-independent) orbits are more complex, and the time-dependent perturbations to which the system is subjected may not be strictly sinusoidal. However, as will be shown in this paper, one might still expect generically that a system exhibiting damped oscillations of the form associated with many scenarios involving collective relaxation will exhibit a large amount of chaos.

That time-dependent perturbations can lead to transient chaos has been recognized already in other branches of physics, including non-neutral plasmas (cf. Qian, Davidson & Chen 1995; Strasburg & Davidson 2000) and charged particle beams (Gluckstern 1994). Indeed, Gluckstern has suggested that chaos triggered by time-dependent perturbations may be responsible for undesirable broadening ('emittance growth') in a focused charged particle beam by ejecting particles from the central core into an outerlying halo.

Section 2 of this paper begins by discussing some 'natural' physical expectations one might have regarding the possibility of transient chaos induced by time-dependent perturbations, and then describes a set of numerical experiments that were performed to test these expectations. Section 3 focuses on the possibility of transient chaos in its purest form, considering in detail what can happen when an integrable spherical system is subjected to an undamped oscillatory perturbation with a single frequency. Section 4 extrapolates from this example to consider more realistic computations that capture two important aspects associated with violent relaxation.

(i) *Allowing for damped oscillations.* Can one trigger efficient chaotic mixing within (say) a period of 10 dynamical times t_{D} or so while simultaneously damping the original strongly time-dependent potential to a nearly time-independent state?

(ii) *Allowing for a variable pulsation frequency.* As the density distribution changes, one might expect that the pulsation frequency will also change, and the obvious question is: do such changes matter significantly?

Section 5 summarizes the principal conclusions and describes extensions of the work described herein currently underway.

2 WHAT WAS EXPECTED AND WHAT WAS DONE

2.1 Physical expectations

As stated already, the basic idea is that an appropriate time-dependence added to a potential can trigger chaos via a parametric resonance: if orbits are subjected to a perturbation with power at appropriate frequencies, one might expect otherwise regular orbits to become chaotic. In particular, if unperturbed orbits have power concentrated at frequencies $\sim\Omega$ and the perturbation has significant power at frequencies ω sufficiently close to Ω, there is the possibility of resonance overlap which, as is well known (cf. Lichtenberg & Lieberman 1992), can lead to the onset of global stochasticity.

As a particularly simple example, one knows that if a regular orbit with substantial power at some frequency Ω is perturbed by a sinusoidal perturbation with frequency $\omega = \Omega$, the orbit will typically exhibit a drastic response that can manifest a sensitive dependence on initial conditions. This is, for example, the physics responsible for resonant circuits in elementary electronics. The real issue, one might argue, is simply: 'how close' must Ω and ω be to trigger strong exponential sensitivity?

A detailed analysis of the effects of resonance overlap suggests generically that the width of such resonances will be an increasing function of amplitude. Even if a slightly 'detuned' small-amplitude perturbation has no apparent effect, a large perturbation with identical frequency may elicit a huge response. Indeed, the numerical models described in Sections 3 and 4 of this paper indicate that, for large-amplitude perturbations – a fractional amplitude of the order of 10–20 per cent or more – the resonance can be very broad. In particular, these models reveal that, if the power in the orbits is concentrated at frequencies $\sim\Omega$, one can obtain a non-trivial increase in chaos – in both the relative number of chaotic orbits and the value of the largest Lyapunov exponent – for sinusoidal perturbations with $0.1\Omega \lesssim \omega \lesssim 30\Omega$. In other words, the resonance can be more than two orders of magnitude wide!

The important point, then, is that if resonances of this sort are really so broad, one might expect transient chaos to be extremely common, if not ubiquitous, in time-dependent galactic potentials. Numerical simulations of galaxy encounters and mergers and most models of galaxy and halo formation imply that a system approaching equilibrium will exhibit damped oscillations. To the extent, however, that one is dealing with collisionless relaxation, there is dimensionally only one natural time-scale in the problem, namely the dynamical time-scale $t_{\mathrm{D}} \sim 1/\sqrt{G\rho}$, where ρ is a characteristic density. In particular, t_{D} should set the oscillation time-scale and the orbital time-scale. The exact numerical values of these time-scales will involve numerical coefficients that will in general be unequal and vary as a function of location within the galaxy. If, however, one only needs to assume that the oscillation and orbital time-scale agree to within an order of magnitude or so, it would seem probable that the conditions appropriate for resonance-induced transient chaos could arise in much, if not all, of the galaxy.

The crucial recognition, then, is that even a relatively short period of exponential sensitivity can result in comparatively efficient chaotic phase mixing. Earlier analysis of flows in time-independent potentials (cf. Mahon et al. 1995; Merritt & Valluri 1996; Kandrup 1998) have demonstrated that the presence of chaos can dramatically enhance the degree to which a system becomes 'shuffled' and, hence, the rate at which a localized orbit ensemble evolves towards an equilibrium. By complete analogy, one might expect that transient chaos in a self-consistently determined time-dependent potential will again enhance the efficacy of 'mixing' and, by so doing, facilitate a more rapid approach towards an equilibrium.

It should be noted explicitly that the physical mechanism for the generation of chaos described here is very different from the mechanism whereby the amount of chaos can increase – or decrease – in more slowly varying potentials (cf.Kandrup & Drury 1998; Contopoulos 2002, private communication). If the potential is slowly varying, one can visualize an orbit as moving in a phase space that

is slowly changing but that is nearly constant over a time-scale $\sim t_{\rm D}$. It is then natural to suppose that at some times the orbit finds itself in a phase space region that is 'chaotic' in the sense that there is a sensitive dependence on initial conditions, but that at other times it finds itself in 'regular' regions where there is no such sensitive dependence. In the setting envisioned in this paper, the phase space is changing on a time-scale comparable to – or even shorter than – the orbital time-scale, so that this picture is necessarily lost. Moreover, in the setting described here one would expect generically a systematic *increase* in the amount and degree of chaos, not simply a change that could be either positive or negative.

Finally, it should be noted that, to a certain extent, the term *transient chaos* is necessarily 'fuzzy'. Chaos, like ordinary Lyapunov exponents, is only defined in an asymptotic $t \rightarrow \infty$ limit. The point, however, is that, even over finite time intervals, it is physically meaningful to ask whether orbits exhibit an exponentially sensitive dependence on initial conditions. This is, for example, the notion that motivates the definition of finite-time Lyapunov exponents (cf. Grassberger, Badii & Politi 1988), which have become accepted tools in non-linear dynamics. From a phenomenological point of view, it makes perfect sense to identify an orbit as exhibiting significant transient chaos if, for some finite time $>t_{\rm D}$, an orbit exhibits significant exponential sensitivity. In many cases, it is clear by visual inspection and/or through a computation of a finite-time Lyapunov exponent whether such transient chaos is present. In other cases, however, things are not so completely clear. For example, for the models considered in this paper it proves difficult to determine with complete reliability a minimum frequency at which transient chaos 'turns on' since this 'turning on' is comparatively gradual.

2.2 Numerical experiments

The numerical computations described in this paper involved perturbations of a Plummer sphere, which is characterized (in units with $G = m = 1$) by the potential

$$V_0(x, y, z) = -\frac{1}{(1 + x^2 + y^2 + z^2)^{1/2}}. \tag{2}$$

This form was selected (i) for its inate simplicity and, especially, (ii) because orbits in this potential are all strictly integrable. Any chaos that is observed can be associated unambiguously with the perturbations that were introduced. These were assumed to take the form

$$V_1(x, y, z, t) = -\frac{m}{(1 + x^2 + a^2y^2 + z^2)^{1/2}}, \tag{3}$$

where the quantities m and a are allowed to vary in time. A variety of different time-dependences were considered, including the following.

(i) Strictly sinusoidal oscillations in m or a, i.e.

$$m = m_0 \sin \omega t \qquad \text{and} \qquad a = a_0 + \delta a \sin \omega t. \tag{4}$$

This allowed one to focus on the physical mechanism in its 'purest' form.

(ii) Sinusoidal oscillations that damp exponentially or as a power law in time, i.e.

$$m = m_0 \mathrm{e}^{-\alpha t} \sin \omega t \tag{5}$$

or

$$m = m_0 \frac{\sin \omega t}{(t_0 + t)^p}, \tag{6}$$

with $p = 1$ or 2, and analogous formulae for $a(t)$. This allowed one to confirm that the physical effects associated with a purely oscillatory perturbation persist if, as is natural in the context of violent relaxation, one allows for a galaxy that damps towards equilibrium.

(iii) Non-oscillatory damping, i.e.

$$m = m_0 \mathrm{e}^{-\alpha t} \tag{7}$$

or

$$m = \frac{m_0}{(t_0 + t)^p} \tag{8}$$

and analogous formulae for $a(t)$. This allowed one to demonstrate that the presence of an oscillatory component is crucial in order to obtain a substantial amount of transient chaos. As will be described below, computations with perturbations given by equation (7) or (8) typically exhibited comparatively minimal amounts of transient chaos.

(iv) Variable driving frequency, assuming that

$$\omega(t) = \omega_0 + \delta(t), \tag{9}$$

with $\delta(t)$ a randomly varying variable that samples an Ornstein–Uhlenbeck process (cf. Van Kampen 1981). What this means is that $\delta$is treated as Gaussian coloured noise, so that its statistical properties are determined uniquely by its first two moments, which are assumed to satisfy

$$\langle \delta(t) \rangle = 0 \quad \text{and} \quad \langle \delta(t_1)\delta(t_2) \rangle = \Delta^2 \exp(-|t_1 - t_2|/t_{\rm c}), \tag{10}$$

where Δ represents the typical 'size' of the random component and $t_{\rm c}$ is the time-scale over which it changes appreciably. Considering perturbations of this form allows one to confirm that, because the resonance is comparatively broad, permitting the driving frequency to drift (within limits) has a relatively minor – albeit potentially significant – effect. This again is important physically. Since the density distribution varies as a galaxy evolves towards an equilibrium, one would anticipate that the characteristic oscillation frequency (or frequencies) would change.

Computations were performed for ensembles of 1600 initial conditions that were generated in two different ways. (i) Broad 'representative' ensembles were generated by uniformly sampling a constant-energy hypersurface. A study of orbits generated from such ensembles allows one to derive systematic effects that might be expected to act in a galaxy as a whole. (ii) Localized ensembles were generated by sampling small phase space hypercubes. Studying orbits generated from such ensembles allows one to determine the extent to which the 'smooth' behaviour associated with the representative ensembles reflects the choice of ensemble as opposed to properties of the resonance.

Most experiments involved perturbations at the 50 per cent level or less, i.e. $m_0 \lesssim 0.5$ and/or $\delta a \lesssim 0.5$. For the intermediate energies considered throughout, a 'typical' orbital frequency (derived from a Fourier transform) was $\Omega \sim 0.3$–0.35, corresponding to $t_{\rm D} = 2\pi/\Omega \sim 20$ in absolute units. On physical grounds one might expect that the perturbations should damp on a time-scale comparable to, but somewhat longer than, $t_{\rm D}$, so that most experiments assumed that (to within factors of a few) t_0 and $\alpha^{-1} \sim 5t_{\rm D} \sim 100$. [Computations of chaotic phase mixing in time-independent potentials (cf. Kandrup & Novotny 2002) typically exhibit an exponential approach towards a near-invariant distribution on a time-scale of $\sim 5\ t_{\rm D}$!]

3 PARAMETRIC RESONANCE AND TRANSIENT CHAOS

Computations involving representative orbit ensembles have led to several unambiguous conclusions.

(i) Integrations that do not involve large-scale time variations on a time-scale $\sim t_{\rm D}$ yield little, if any, transient chaos. In particular, as will be illustrated more carefully in the following section, allowing for non-oscillatory damped perturbations of the form given by equation (7) does not result in large measures of chaos, even for large amplitudes $m_0 \gtrsim 0.5$. However, allowing for oscillations in m and/or a *can* trigger substantial amounts of chaos.

(ii) There are at least two solid reasons to believe that this chaos is triggered by a resonance. More obvious, perhaps, is the fact that the largest increases in chaos – as reflected by both the number of chaotic orbits and the size of a typical Lyapunov exponent – arise for driving frequencies comparable to, or somewhat larger than, the frequencies for which the unperturbed orbits have most of their power. Equally significant, however, is the fact that the driving frequencies that result in the greatest amount of chaos correspond precisely to those frequencies for which the orbital energies are 'shuffled' the most, i.e. where different particles with the same initial energy end up with the largest spread in final energies. A priori there need be no direct connection between increases in chaos and large-scale shuffling of energies. However, one *would* expect resonant couplings to lead to significant changes in energies. A correlation between changes in energy and the amount of chaos thus corroborates the interpretation that this chaos is resonant in origin.

(iii) At least for the case of large-amplitude oscillations, $m_0 \gtrsim 0.1$ or so, the resonance is comparatively broad. One observes significant increases in both the relative measure of chaotic orbits *and* the size of the largest Lyapunov exponent whenever the driving frequency ω and the natural orbital frequencies Ω agree to within an order of magnitude or so. If, for example, one considers an energy where the natural frequencies peak for $\Omega_m \sim 0.3$–0.35 or so, noticeable increases in the degree of chaos are observed for $0.035 \lesssim \omega \lesssim 10.0$, i.e. $0.1 \sim \omega/\Omega_m \sim 30$.

(iv) The width of the resonance, i.e. the range of values of ω for which one sees an appreciable increase in the degree of chaos, appears to be an increasing function of amplitude.

(v) The resonance appears to be smooth in the sense that, for fixed amplitude, the relative number of chaotic orbits and the size of the largest Lyapunov exponent both vary smoothly as functions of the driving frequency ω. In particular, plots of the fraction f of the orbits that are chaotic or the mean size $\langle\chi\rangle$ of the largest Lyapunov exponent as functions of driving frequency typically exhibit a single peak. There is no obvious evidence for complex structure within the resonance.

(vi) For fixed ω, the relative number of chaotic orbits and the size of the largest Lyapunov exponent are both an increasing function of perturbation amplitude, although it appears that the fraction f of orbits that are chaotic can asymptote towards a fixed value f_M for sufficiently large amplitudes. For some values of ω, especially those near the centre of the resonance, this f_M can approach unity; for other choices of frequency, f_M can be substantially smaller.

(vii) Whether or not the perturbation breaks spherical symmetry appears to be relatively unimportant, e.g. making the parameter a time-dependent or otherwise different from unity does not change things all that much. Provided that the system manifests large-amplitude oscillations, one can apparently obtain just as much chaos for spherical systems as for non-spherical systems.

Evidence for several of these conclusions is provided in Figs 1–4 (see below), all generated from the same set of 1600 initial conditions, evolved for a total time $t = 512$ in the presence of a strictly sinusoidal perturbation of the form given by equation (4) with $a \equiv 1$. The two panels of Fig. 1 exhibit the relative measure f of chaotic orbits as a function of driving frequency ω for five different choices of amplitude m_0. The top panel exhibits $f(\omega)$ on a linear scale, thus allowing one to focus on the behaviour of the resonance at higher frequencies; the lower exhibits f as a function of $\log_{10}\omega$, which allows one to see more clearly the behaviour at lower frequencies.

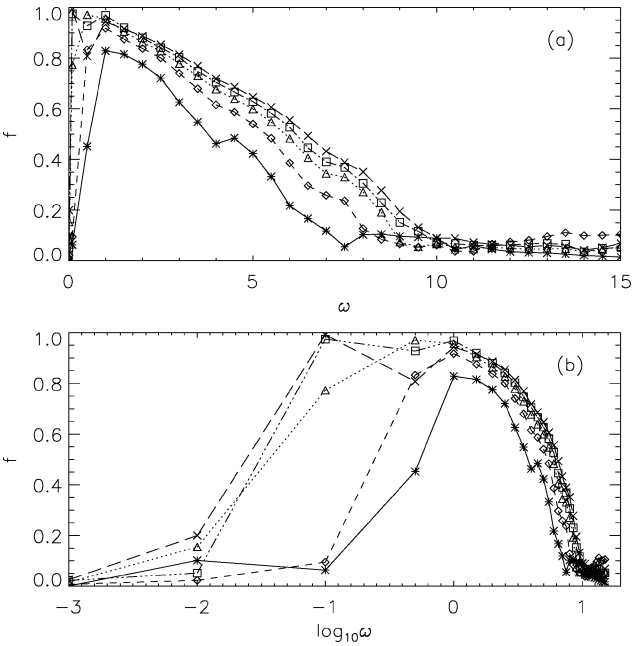

Figure 1. (a) The relative fraction f of chaotic orbits in a representative 1600 orbit ensemble that are subjected to strictly sinusoidal oscillations with variable frequency ω. The different curves represent, from bottom to top, driving amplitudes $m_0 = 0.1$, 0.2, 0.3, 0.4 and 0.5. (b) The same data plotted as a function of $\log_{10}\omega$.

Most obvious, perhaps, from Fig. 1 is the fact that the width of the resonance is an increasing function of m_0, although this increase appears to be comparatively small for $m_0 > 0.2$ or so. Also evident is the fact that, except perhaps for the lowest amplitude, $m_0 = 0.1$, the fraction f appears to vary smoothly with frequency. In each case, f peaks at a frequency $\omega_{\rm max}$ comparable to the typical natural frequencies $\Omega \sim 0.3$–0.35 associated with the unperturbed orbits. However, $\omega_{\rm max}$ *does* seem to vary somewhat as a function of m_0. For larger amplitudes, near $\omega_{\rm max}$ essentially all the orbits are chaotic, i.e. $f(\omega_{\rm max}) \approx 1$. For lower frequencies $f(\omega_{\rm max})$ can be significantly less than unity. Overall, there is evidence for significant amounts of transient chaos for $0.35 \lesssim \omega \lesssim 10.0$.

The two panels of Fig. 2 exhibit $\langle\chi\rangle$, the mean value of the largest finite-time Lyapunov exponent for the same ensembles, again plotted on both linear and logarithmic scales. Here $\langle\chi\rangle$ was extracted by first identifying those orbits in the ensemble that were deemed chaotic and then computing the mean value of χ for those orbits.

Fig. 3 exhibits δE, the root mean squared spread in energies at time $t = 512$ for the chaotic orbits identified in Figs 1 and 2. It is clear visually that, as one would expect if the transient chaos is associated with a resonant coupling, the frequencies that result in the largest measures of chaotic orbits and the largest $\langle\chi\rangle$ also result in the largest shifts in energy. However, it is also evident that, especially for the higher-amplitude perturbations, δE exhibits a more complex dependence on ω than do $f(\omega)$ or $\langle\chi(\omega)\rangle$. This does not contradict the assertion that transient chaos is induced by a resonant coupling, but it *does* suggest that the amount and degree of chaos in the broad resonance region is less sensitive to the pulsation frequency than is the

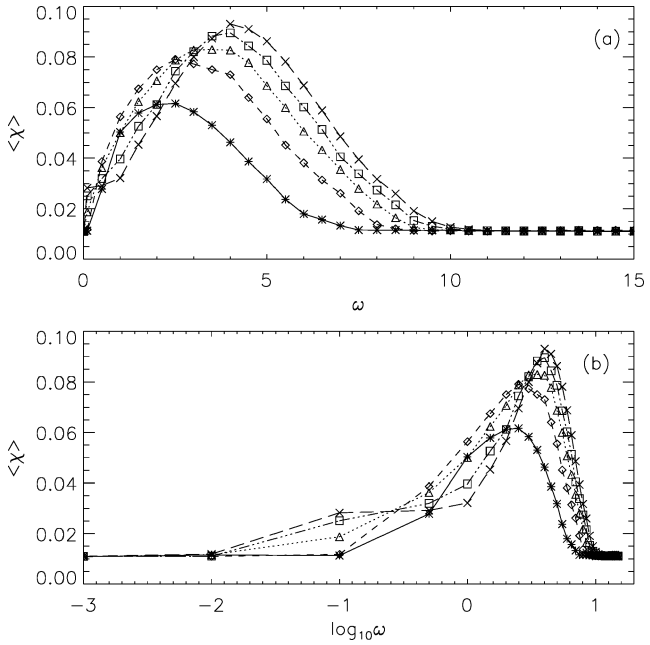

Figure 2. (a) The mean value $\langle\chi\rangle$ of the chaotic orbits in the ensembles used to generate the preceding figure, again plotted as a function of ω. (b) The same data plotted as a function of $\log_{10}\omega$.

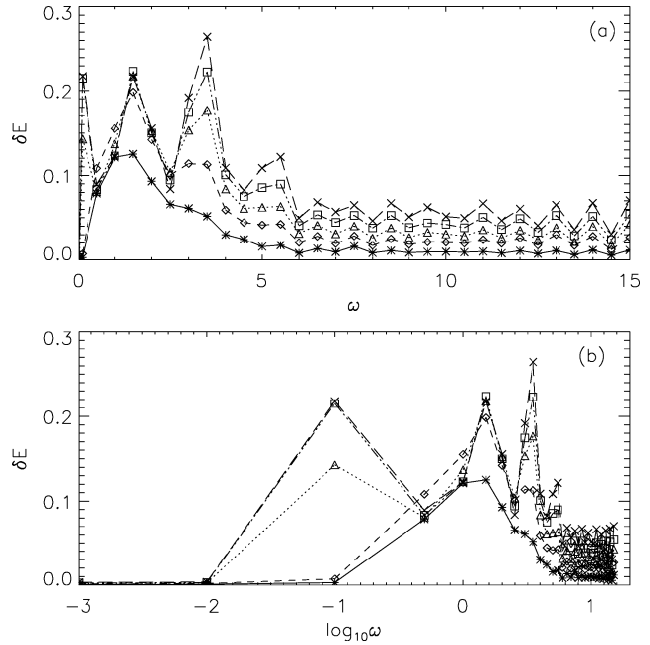

Figure 3. (a) The root mean squared spread in energies, $\delta E_{\rm rms}$ ($t = 512$), for the orbit ensembles used to generate the first two figures. (b) The same data plotted as a function of $\log_{10}\omega$.

shuffling in energies. This has potentially significant implications for violent relaxation, where one is interested in both (i) shuffling the energies of the individual masses and (ii) randomizing their phase space locations on a constant energy hypersurface.

One other point is also evident from this figure, namely that, at least for frequencies well into the resonance, the spread in energies can be very large. This reflects the fact that, because of the resonant coupling, a significant fraction of the orbits have acquired large energies that set them along trajectories involving excursions to very large radii, $r > 10$ or more. Allowing for a resonance that is this strong to last for as long as $t \approx 20t_{\rm D}$ is completely unrealistic in the context of any model for violent relaxation. The computations described in Section 4.2, which incorporate strong damping, avoid this artificial behaviour.

In part because of this effect, any uniform prescription used to distinguish between 'regular' and 'chaotic' orbits is necessarily somewhat ad hoc and, as such, fraught with difficulties. Figs 1 and 2 reflect an analysis in which 'chaotic' was defined as corresponding to a finite-time Lyapunov exponent for the interval $0 < t < 512$ with a value $\chi \geqslant 0.012$, arguably a fairly large threshold value. Lowering the threshold value of 0.012 to a smaller value would of course increase the estimated fraction f of chaotic orbits and decrease the mean value of $\langle\chi\rangle$ for those orbits deemed chaotic. In any event, the choice $\chi \geqslant 0.012$ implies that there is little if any chaos for $\omega \lesssim 0.01$ and $\omega \gtrsim 10$, which is consistent with the fact that localized ensembles exhibit little if any evidence of chaotic phase mixing for $\omega < 0.01$ and $\omega > 10$ or so. Despite this, however, it should be recognized explicitly that this prescription really identifies orbits that are 'obviously' or 'strongly' chaotic, and that it may be ignoring a considerable number of orbits that are only very weakly chaotic.

This prescription, as for any other that involves a fixed minimum value and a fixed integration time, is open to criticism. For those frequencies and amplitudes where the resonance is especially strong and many orbits quickly achieve large energies, it might seem more appropriate to consider a shorter time interval, during which the orbits are restricted to smaller radii. However, for frequencies and amplitudes for which the resonance is weaker, one might wish instead to integrate for much longer times so as (hopefully) to allow for clear distinctions to be made between regular and 'extremely sticky', nearly regular (cf. Contopoulos 1971) orbits. The choice of a time interval $t = 512$ represents a compromise necessitated by the idealized nature of the computations described in this section.

In any event, what is inevitable is that, for chaotic orbits in any potential, one must expect correlations between the energy of the orbit and the size of a typical finite-time Lyapunov exponent χ. For the potential considered here, one finds typically that the orbits deemed regular are precisely those that exhibit the smallest changes in energy and hence, overall, the smallest excursions from the origin. However, for those orbits that *are* chaotic, those spending more time at larger radii and that, for this reason, have larger orbital time-scales, tend to have somewhat smaller values of χ.

Fig. 4 exhibits the relative measure of chaotic orbits as a function of amplitude m_0 for three different frequencies, namely $\omega = 1.4$, 3.5 and 7.0. For $\omega = 1.4$, a frequency in the middle of the resonance, for amplitudes as large as $m_0 = 0.25$ almost all the orbits exhibit evidence of chaos. For $\omega = 3.5$, a value somewhat closer to the edge of the resonance, the relative abundance of chaotic orbits is somewhat smaller. However, for $m_0 = 0.25$ as many as 75 per cent of the orbits are clearly chaotic, a fraction that does not increase significantly if m_0 is increased. For $\omega = 7.0$, a value near the edge of the resonance, the fraction of the orbits that is chaotic is smaller and does *not* appear to level off for $m_0 > 0.25$ or so. Indeed, if the amplitude is increased to a value as large as $m_0 = 1.0$ as many as 50 per cent of the orbits prove chaotic, i.e. $f(m_0 = 1) \approx 0.5$.

The uniform criterion used to identify chaotic orbits for Figs 1 and 2 fails for $m_0 \lesssim 0.1$. For that reason, Fig. 4 implemented a different, somewhat more subjective criterion that has been used successfully in distinguishing between regular and 'very sticky' chaotic orbits in the triaxial generalizations of the Dehnen potentials (Siopis & Kandrup 2000). What this entailed was ordering the 1600 computed

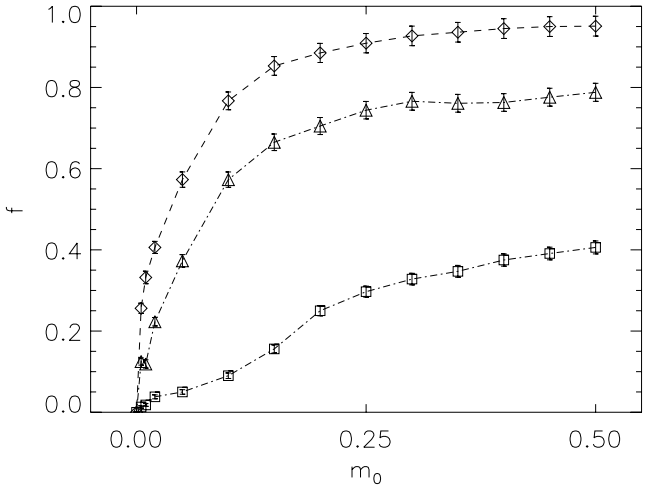

Figure 4. The relative fraction f of chaotic orbits in a representative 1600 orbit ensemble that are subjected to strictly sinusoidal oscillations of the form given by equation (4) of variable amplitude m_0 with $\omega = 1.4$ (upper curve), $\omega = 3.5$ (middle curve) and $\omega = 7.0$ (lower curve).

values of χ at various times T_A, plotting the ordered list of $\chi(T_A)$ values for different values of T_A, and then in each case searching for a 'kink' in the curve. This prescription appears to permit an accurate determination of a fraction f of the orbits exhibiting chaotic behaviour that is insensitive to the precise choice of T_A, although the estimated size of the finite time $\chi(T_A)$ *does* depend on the sampling interval.

Additional insights into the nature of the resonance can be derived from Fig. 5, which shows the x-components of the composite (normalized) Fourier transforms of coordinate and force per unit mass, $|x(\Omega)|$ and $|a_x(\Omega)|$, constructed by combining spectra for 1600 unperturbed $\omega = 0$ orbits generated from the same initial conditions used to generate Figs 1–3. (Because of spherical symmetry the y- and z-components are statistically identical.) As noted already, for this particular choice of energy, $|x(\Omega)|$ peaks at $\Omega_m \sim 0.3$–0.35 and is comparatively negligible for much higher and lower frequencies. In contrast, $|a_x(\Omega)|$ has multiple peaks associated with higher-frequency harmonics that arise because the force per unit mass is a non-linear function of position. It is natural to suppose that it is these harmonics that are responsible for the comparatively large responses at frequencies Ω that are large compared with Ω_m, which are evident in Figs 1–3. It is particularly interesting that this response cuts off for driving frequencies ω that are large compared with 2Ω, rather than Ω, a fact that would suggest that one is observing the effects of a broad 2:1 resonance similar to that arising in the standard Matthieu equation (see, e.g., Matthews & Walker 1964).

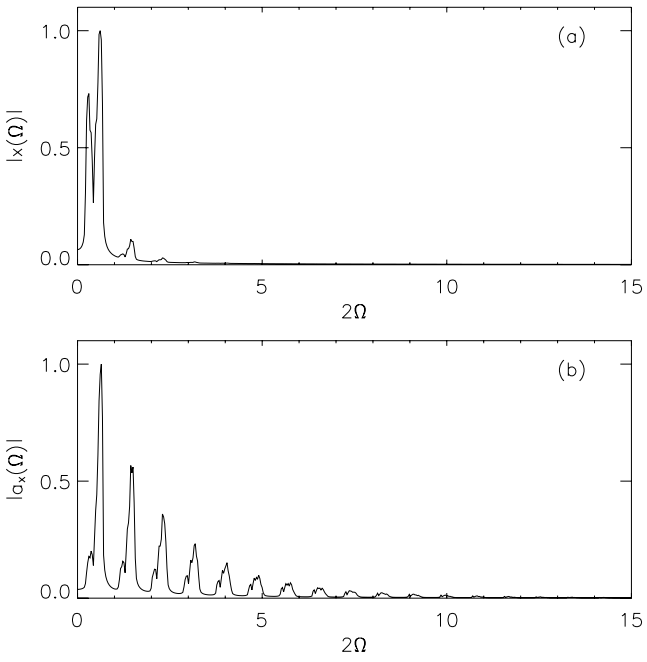

Figure 5. (a) The power spectrum $|x(\Omega)|$ associated with the x-component of the orbits generated from the 1600 initial conditions used to created Figs 1–3, evolved in the absence of any time-dependent perturbation and plotted as a function of 2Ω. (b) The power spectrum $|a_x(\Omega)|$ associated with the x-component of the force per unit mass associated with the same orbits.

Much of the smoothness in plots such as those given in Fig. 2 reflects the fact that the data were generated from 'representative' ensembles of initial conditions. If the same analysis is repeated for different localized ensembles of initial conditions, even ensembles with the same energy, one observes significant variability in both the size of a typical finite-time Lyapunov exponent and the value of the frequency ω for which $\langle\chi\rangle$ is maximized. And similarly, plots of quantities such as $\langle\chi\rangle$ as a function of ω for such ensembles exhibit more structure than do plots for representative ensembles. This presumably reflects the fact that the natural frequencies of the otherwise regular orbits vary with phase space location, and that some frequencies are more susceptible to the resonance than others. This additional structure could have important implications for near equilibria subjected to nearly periodic perturbations, which could impact certain orbits much more than others. However, one might expect that, when considering the 'global' properties of violent relaxation, such details would tend to wash out.

4 A TOY MODEL FOR VIOLENT RELAXATION

4.1 Variable pulsation frequencies

Allowing for a randomly varying frequency of the form given by equations (9) and (10) leads to several significant conclusions.

(i) Perhaps the most important is that allowing for a comparatively slow frequency drift can actually *increase the relative measure of chaotic orbits.* Suppose that the unperturbed frequency ω_0 is well into the resonant region and that Δ is not sufficiently large to push ω outside. In this case, the introduction of a perturbation $\delta(t)$ with an autocorrelation time t_c that is long compared with t_D tends to convert many, if not all, the 'regular' orbits into orbits with an appreciable exponential sensitivity. This behaviour can be understood by supposing that, in the absence of the frequency drift, there exist some regular orbits which, because of the particular values of their natural frequencies, barely manage to avoid resonating with the perturbation. Allowing for a drift facilitates an improved resonance coupling that can make (some of) these orbits chaotic for at least some of the time.

(ii) Provided that ω_0 and $\omega_0 \pm \Delta$ are well within the resonance region, it is also apparent that, as the autocorrelation time t_c decreases, the degree of chaos, as probed by the mean $\langle\chi\rangle$, tends to decrease, even though the relative fraction of chaotic orbits may well remain equal to unity.

(iii) For fixed autocorrelation time t_c, the mean $\langle\chi\rangle$ manifests only a relatively weak dependence on Δ, at least for $0.1 \lesssim \Delta/\omega_0 \lesssim 0.8$. For some choices of t_c increasing Δ causes an increase in the

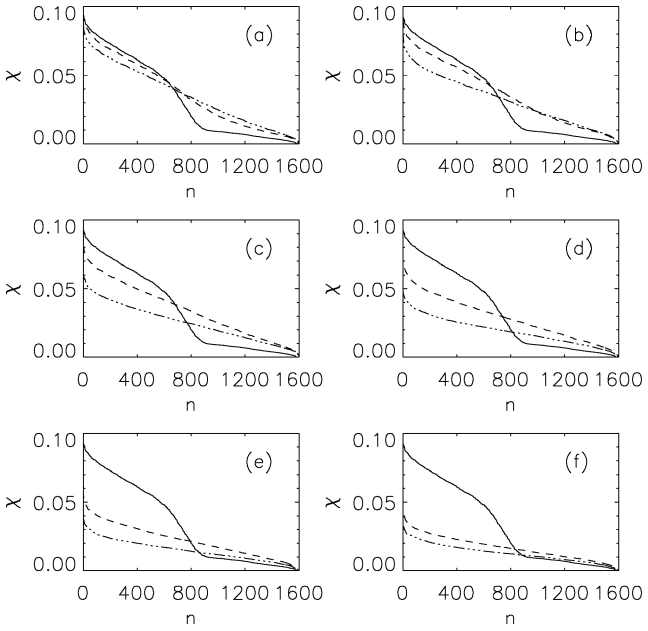

Figure 6. (a) Finite-time Lyapunov exponents for 1600 representative orbits evolved for a time $t = 512$ in an undamped Plummer potential pulsed with amplitude $m = 0.1$ and a frequency $\omega(t) = \omega_0 + \delta(t)$, with $\omega_0 = 3.5$, autocorrelation time $t_c = 320 = 16t_D$, and $\Delta^2 = 0.35$ (dashed curve) and $\Delta^2 = 2.8$ (triple-dot-dashed). The solid curve contrasts exponents derived for an evolution with $\delta \equiv 0$. (b) The same for $t_c = 160$, (c) $t_c = 80$, (d) $t_c = 40$, (e) $t_c = 20$ and (f) $t_c = 10$.

mean finite-time χ; in other cases increasing Δ decreases the mean. However, the observed variations are invariably small.

All three of these points are illustrated in Figs 6 and 7. The dashed and triple-dot-dashed curves in Fig. 6 correspond to plots of ordered finite-time Lyapunov exponents χ associated with 1600 initial conditions subjected to undamped pulsations with variable frequency $\omega = \omega_0 + \delta(t)$ for $m_0 = 0.1$, $\omega_0 = 3.5$ and different choices of Δ and t_c. The solid curve in each panel contrasts the exponents generated for the same initial conditions evolved with $\delta = 0$. It is evident that, for the largest values of t_c, the differences between the curves with δzero and non-zero are relatively small, at least for the largest values of χ. However, it is also apparent that the time-dependent frequency drift has significantly reduced the relative number of orbits with very small finite-time χ values. Also evident is the fact that decreasing the autocorrelation time t_c, i.e. making the frequency drift more quickly, tends generically to decrease the typical value of χ, although the relative measure of chaotic orbits may not change appreciably. For this particular choice of ω_0 and m_0, increasing Δ for fixed t_c also tends to reduce the typical size of a finite-time χ. This, however, is *not* generic. If, instead, the same computations are repeated for $m_0 = 0.05$, one finds that the choice of Δ that leads to the largest χ values actually varies with t_c.

The effects of varying Δ and t_c on the mean $\langle\chi\rangle$ and the dispersion σ_χ associated with these ensembles is exhibited in Fig. 7.

4.2 Damped oscillations

Allowing for damped oscillations of the form given by equation (5) or (6) has a comparatively minimal effect. Not surprisingly, the size of the mean Lyapunov exponent $\langle\chi\rangle$ decreases as time elapses and there can be a gradual decrease in the relative fraction f of orbits

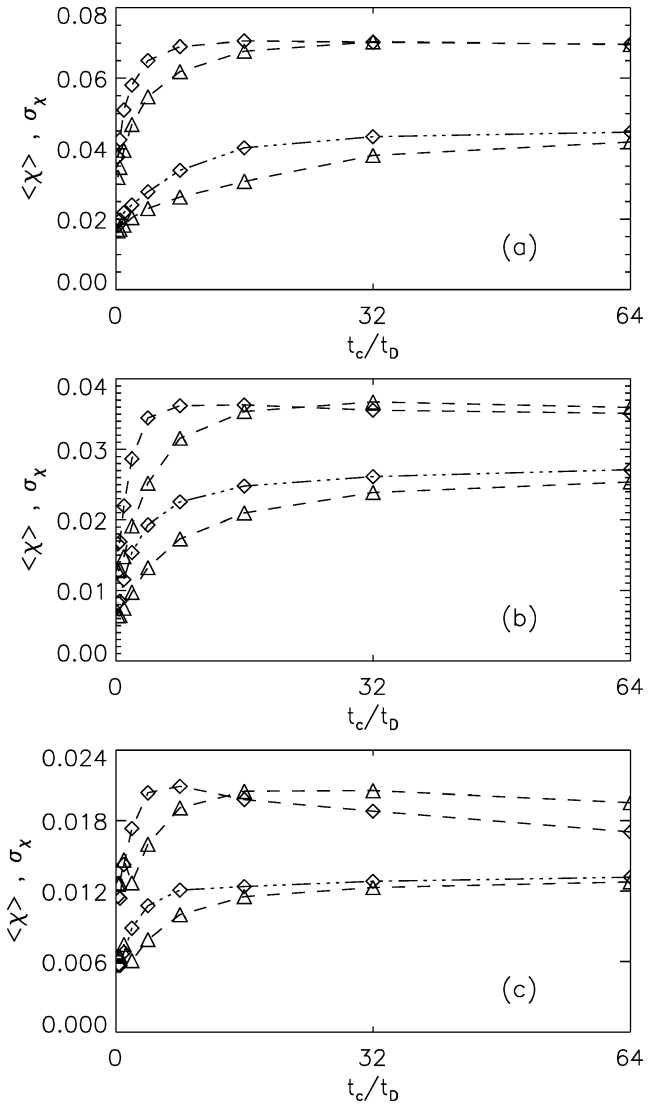

Figure 7. (a) The mean Lyapunov exponent $\langle\chi\rangle$ (upper two curves) and the associated dispersion σ_χ (lower two curves) computed for ensembles of 1600 orbits evolved in an undamped Plummer potential with amplitude $m = 0.5$, $\omega_0 = 3.5$ and variable autocorrelation time t_c. Diamonds correspond to $\Delta^2 = 0.35$, triangles to $\Delta^2 = 2.8$. (b) The same for $m_0 = 0.1$, (c) $m_0 = 0.05$.

exhibiting exponential sensitivity. However, the basic phenomenon of transient chaos persists until the perturbation has damped almost completely away.

This is evident from Fig. 8, which was again generated from the same 1600 initial conditions used to generate Figs 1–5, now allowing for a perturbation of the form given by equation (6) with $m_0 = 0.5$, $t_0 = 100$ and $p = 2$, again allowing for variable ω. Here the four lower curves (from top to bottom) represent mean values of the finite-time Lyapunov exponent $\langle\chi\rangle$ generated separately for the intervals $100 < t < 200$, $200 < t < 300$, $300 < t < 400$ and $400 < t < 500$. The top curve, reproduced from Fig. 2, represents $\langle\chi\rangle$ for $0 < t < 512$ for the same orbits evolved in the presence of undamped ($p = 0$) oscillations with the same initial m_0. It is evident that, as one would have expected, the degree of exponential sensitivity decreases with time and that, by the end of the integration, the orbits are behaving in a nearly regular fashion. The fact that the peak

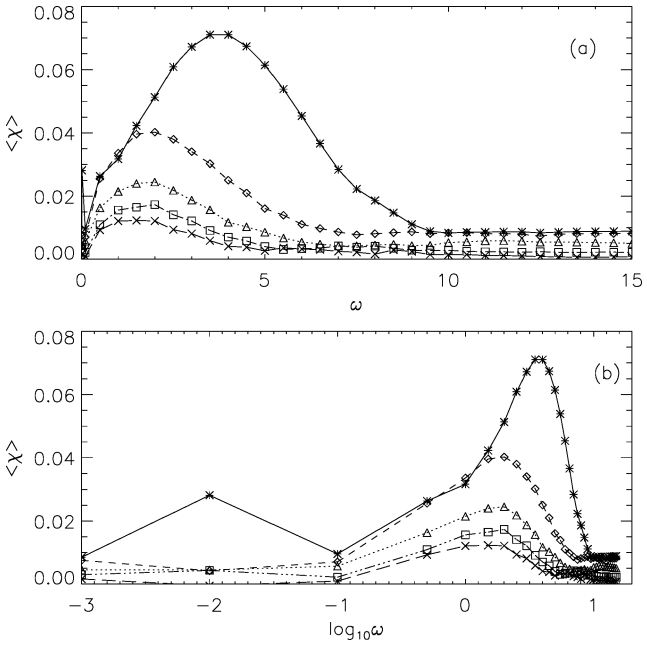

Figure 8. (a) The four lower curves exhibit the mean value $\langle\chi\rangle$ as a function of ω for chaotic orbits subjected to damped oscillations with $m_0 = 0.5$, $p = 2$ and t_0 for the intervals (from top to bottom) $100 < t < 200$, $200 < t < 300$, $300 < t < 400$ and $400 < t < 500$. The top curve exhibits $\langle\chi\rangle$ for undamped ($p = 0$) oscillations for the intervals $0 < t < 512$. (b) The same data plotted as a function of $\log_{10}\omega$.

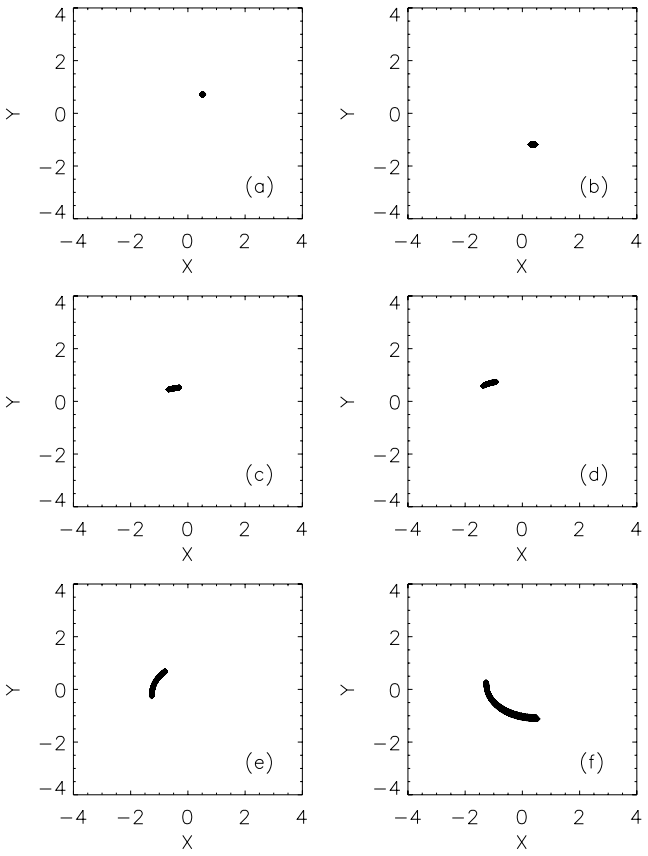

Figure 9. The x and y coordinates of an initially localized ensemble of orbits evolved in a Plummer potential subjected to a non-oscillatory perturbation of the form given by equation (7) with $m_0 = 0.5$ and $p = 2$. (a) $t = 0$. (b) $t = 16$. (c) $t = 32$. (d) $t = 64$. (e) $t = 128$. (f) $t = 256$.

frequency ω drifts towards lower values at later times is consistent with the fact, evident from Fig. 2, that for undamped oscillations, lower amplitudes m_0 correlate with lower values of ω.

That it may be possible to achieve efficient chaotic phase mixing in an oscillating galactic potential while still relaxing towards a nearly integrable state within 10–20$t_{\rm D}$ or so is illustrated visually in Figs 10–12 (see below), which exhibit the behaviour of the same localized ensemble of 1600 initial conditions, again subjected to damped oscillations of the form given by equation (6) with $m_0 = 0.5$, $p = 2$ and $t_0 = 100$ for three different choices of frequency ω. Fig. 9 exhibits the results of a corresponding evolution in the presence of a non-oscillatory perturbation of the form given by equation (8). In each case, the six panels exhibit the x and y coordinates of each of the orbits at times $t = 0$, 16, 32, 64, 128 and 256, the latter corresponding to an interval of approximately $12.8t_{\rm D}$.

It is evident visually from Fig. 9 that, in the absence of oscillations, mixing is comparatively inefficient. Indeed, the evolution in that figure is qualitatively identical to examples of regular phase mixing in time-independent potentials (cf. fig. 2 in Kandrup 1999). As asserted in Section 3, a non-oscillatory perturbation of the integrable Plummer potential leads to little if any transient chaos and, as such, no evidence for chaotic phase mixing. The remaining three figures, which incorporate a systematic pulsation, all yield phase mixing that is substantially more efficient. Fig. 10, which represents orbits that have been pulsed with $\omega = 0.035$, a frequency near the lower edge of the resonance, clearly exhibits more robust mixing, although the mixing is still considerably less efficient than what is observed for strongly chaotic flows in time-independent potentials (cf. fig. 1 in Kandrup 1999). Indeed, it is difficult to determine unambiguously whether the orbits used to generate this figure genuinely exhibit significant transient chaos.

In contrast, Fig. 11, which was generated for $\omega = 0.70$, exhibits precisely the sort of behaviour that one has come to associate with chaotic phase mixing in time-independent potentials. For the first two dynamical times, the localized ensemble of orbits, which started with a phase space size $<10^{-2}$, still remains confined. By $t = 64$, however, corresponding to an interval $\approx 3.2t_{\rm D}$, the orbits have begun to spread significantly; and, by $t = 128$, corresponding to roughly $6.4t_{\rm D}$, the ensemble has dispersed to fill a large portion of the available phase space. Nevertheless, despite this efficient mixing, the potential is damping rapidly towards a near integrable state. By a time $t = 256$, the overall amplitude of the perturbation, $m_0/(1 + t/t_0)^2$, has decreased from $m_0 = 0.5$ to $m_0 \approx 0.04$, this corresponding to a much more nearly time-independent system.

Fig. 12 exhibits an example of 'incomplete' chaotic phase mixing for the case of a frequency $\omega = 3.5$. Here again one sees clear evidence of the dispersive behaviour indicative of chaotic phase mixing; but, since one is closer to the upper edge of the resonance, the efficient mixing has de facto turned off before the ensemble could fill all the accessible phase space. The dearth of orbits near $x = y = 0$ is exactly what one would expect in a time-independent spherical potential for orbits with an appreciable angular momentum.

5 DISCUSSION

The numerical computations described herein lead to several seemingly unambiguous conclusions.

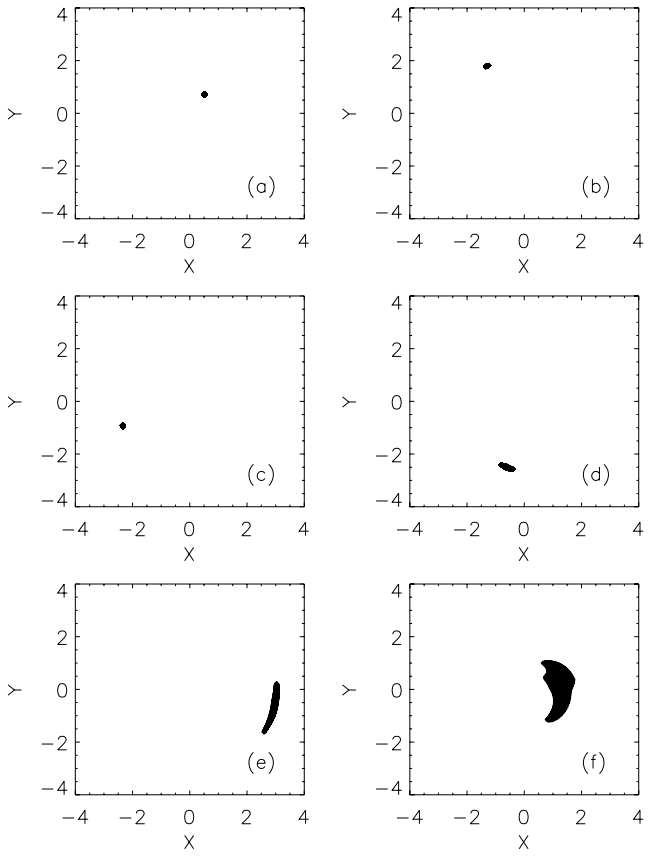

Figure 10. The same as the preceding figure, now allowing for an oscillatory perturbation of the form given by equation (6) with $M_0 = 0.5$, $p = 2$ and $\omega = 0.035$.

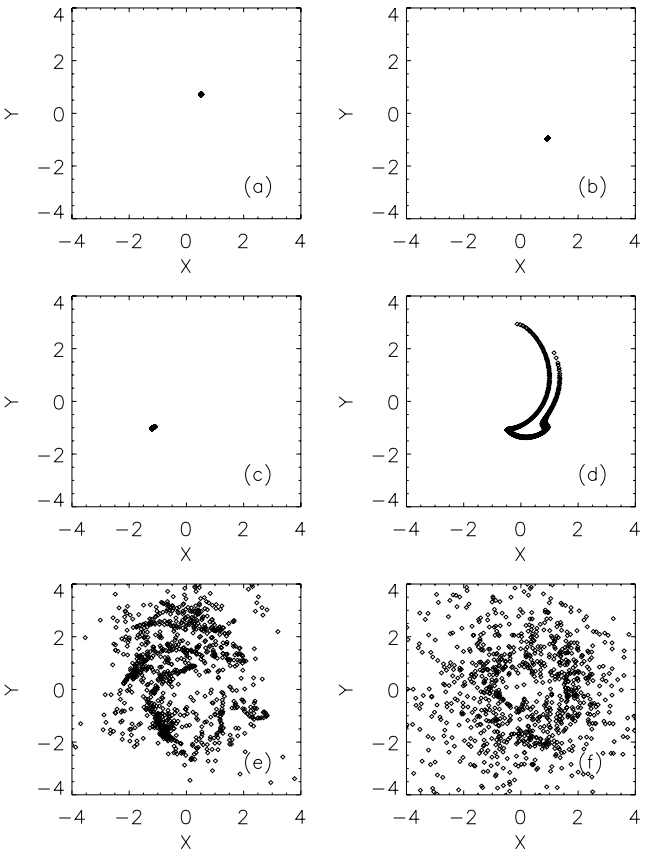

Figure 11. The same as the preceding figure, for $\omega = 0.70$.

(i) Subjecting orbits to a possibly damped oscillatory time-dependence can give rise to substantial amounts of transient chaos, even if the initial and final form of the potential is completely integrable.

(ii) This transient chaos appears to arise from a resonant coupling that, at least for large amplitudes, is very broad and, as such, might be expected to be present in many physical systems.

(iii) This transient chaos can drive chaotic phase mixing, which, in the context of a fully self-consistent evolution, might be expected to play an important role in violent relaxation, e.g. during the formation of galaxies and galaxy haloes and in mergers/close encounters of galaxies.

Three extensions of this work are underway. The first involves a consideration of additional examples with the aim of determining the extent to which this transient chaos is generic. The examples described here suggest that transient chaos can arise whenever the perturbation has substantial power at frequencies that are comparable to within an order of magnitude or so to the natural frequencies associated with the orbits. However, this needs to be checked in the context of other, more realistic models.

A second extension involves efforts to better understand the origins of this chaos using geometric arguments due originally to Pettini (1993). Recently, Kandrup, Sideris & Bohn (2002) showed that thermodynamic arguments proposed originally to predict the size of the largest Lyapunov exponent in high-dimensional time-independent Hamiltonian systems (Casetti, Clementi & Pettini 1996) also work surprisingly well in lower-dimensional (e.g. two- and three-degree-of-freedom) systems. The aim is to adapt that work to the case of Hamiltonian systems admitting a time-dependence of the form that one might expect to encounter in the context of violent relaxation.

The third extension involves searching for evidence of transient chaos in the context of fully self-consistent numerical simulations, both for self-gravitating systems and for non-neutral plasmas, e.g. charged particle beams. Recent simulations (e.g. Kishek et al. 2001) have shown that fully self-consistent simulations of beams can exhibit evidence of chaotic phase mixing. The obvious issue is whether, as one might expect, the degree of chaotic mixing observed in such a beam or in a simulation of violent relaxation in a self-gravitating system correlates with the degree to which the bulk potential admits a significant time-dependent oscillatory component.

Plummer spheres do not constitute especially realistic models of early-type galaxies: aside from the idealization of spherical symmetry, real galaxies often have a central cusp and their densities fall off much more slowly at large radii. Despite this, however, it is interesting to estimate more carefully the 'real' values that Ω and ω might assume if nature did somehow construct Plummer spheres.

To estimate a reasonable value for the pulsation frequency one can proceed as follows: in the dimensionless units used in this paper, the half-mass radius $r_{\rm h}$ inside of which half the mass of the galaxy is contained satisfies $r_{\rm h} \approx 1.3$. However, $\overline{r}(E)$, the mean radius associated with a uniform sampling of an E =constant hypersurface, satisfies $\overline{r}(E) = r_{\rm h}$ for $E \approx 0.4$. One might thus argue that a 'typical' frequency associated with the system as a whole would correspond to a characteristic frequency associated with orbits having $E \sim 0.4$ which, by analogy with Fig. 5, can be computed as $\Omega_m \sim 0.4$. Alternatively, given that the density $\rho = (3/4\pi)(1 + r^2)^{-5/2}$, it is easily

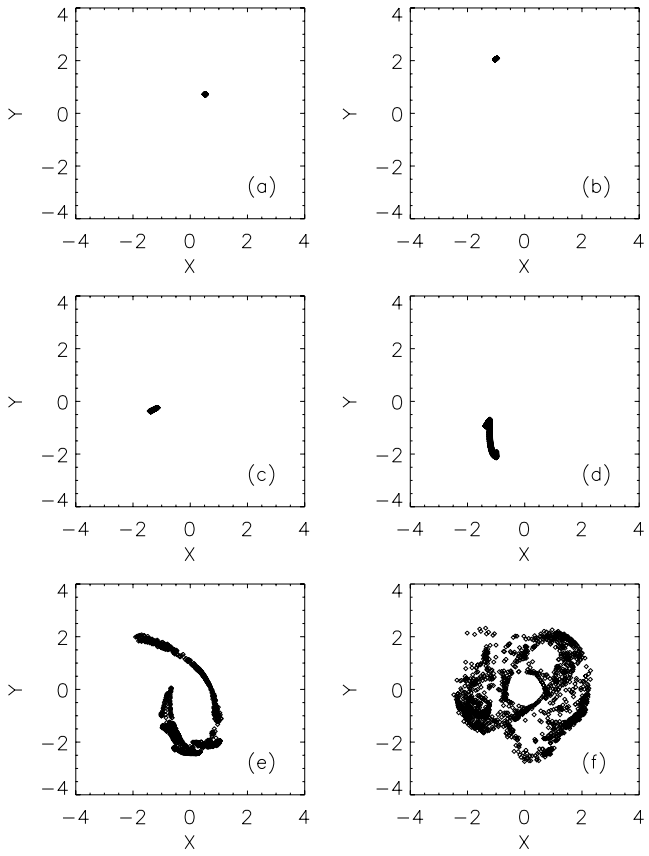

Figure 12. The same as the preceding figure, for $\omega = 3.50$.

seen that the half mass density $\rho_{\rm h} = \rho(r_{\rm h})$ defines a characteristic frequency $\Omega_{\rm h} = \sqrt{4u\pi G\rho_{\rm h}} \approx 0.50$. One might, therefore, anticipate that realistic bulk oscillations associated with the system would be characterized by frequencies $0.4 \lesssim \omega \lesssim 1.0$, with the larger values corresponding to 'higher-order modes'. Alternatively, an examination of Fourier spectra for representative orbit ensembles at different energies shows that the peak frequency ranges from $\Omega_m \rightarrow 1.0$ for $E \rightarrow -1.0$ to, for example, $\Omega_m \sim 0.05$ for $E = -0.1$.

To the extent that the resonance described in this paper is representative of the Plummer sphere, it would thus seem probable that all but the very highest-energy orbits would, in fact, be able to resonate with a large-scale 'bulk' oscillation. One might also be tempted to conclude that the possibility of resonances for $\omega \gg \Omega_m$ is largely unimportant physically. This, however, is not necessarily the case. One anticipates generically that, as the system 'relaxes', power will cascade from larger scales and lower frequencies to shorter scales and higher frequencies. To the extent, however, that the natural frequency of the perturbation is more important than its detailed form, one might expect that such higher-frequency oscillations, once triggered, could play an important role in continuing the process of violent relaxation on shorter scales. This is consistent with the fact (Kandrup et al. 2003) that shorter scale perturbations associated with supermassive black hole binaries orbiting near the centre of a galaxy can trigger qualitatively similar effects in terms of resonant phase mixing and energy and mass transport.

ACKNOWLEDGMENTS

The authors acknowledge useful discussions with Balša Terzić. HEK and IVS were supported in part by NSF AST-0070809. IVS was also supported in part by Department of Education grant G1A62056.

REFERENCES

Binney J., 1978, Comment. Astrophys., 8, 27
Casetti L., Clementi C., Pettini M., 1996, Phys. Rev. E, 54, 5969
Contopoulos G., 1971, AJ, 76, 147
Gluckstern R.L., 1994, Phys. Rev. Lett., 73, 1247
Grassberger P., Badii R., Politi A., 1988, J. Stat. Phys., 51, 135
Kandrup H.E., Sideris I.V., Terzic B., Bohn C.L., 2003, ApJ, submitted
Kandrup H.E., 1998, MNRAS, 301, 960
Kandrup H.E., 1999, in Merritt D., Sellwood J.A., Valluri M., eds, ASP Conf. Ser. Vol. 182, Astron. Soc. Pac., San Francisco, p. 197
Kandrup H.E., 2001, in Ossipkov L.P., Nikiforov I.I., eds, Stellar Dynamics: from Classic to Modern. St Petersburg State Univ., St Petersburg, p. 213
Kandrup H.E., Drury J., 1998, Ann. N.Y. Acad. Sci., 867, 306
Kandrup H.E., Mahon M.E., 1994, Phys. Rev. E, 49, 3735
Kandrup H.E., Novotny S.J., 2002, preprint (astro-ph/0204019)
Kandrup H.E., Pogorelov I.V., Sideris I.V., 2000, MNRAS, 311, 719
Kandrup H.E., Sideris I.V., Bohn C.L., 2002, Phys. Rev. E, 65, 016214
Kishek R.A., Bohn C.L., Haber I., O'Shea P.G., Reiser M., Kandrup H.E., 2001, in Lucas P., Weber S., eds, Proc. 2001 IEEE Particle Accelerator Conf. IEEE Press, Chicago, p. 151
Lichtenberg A.J., Lieberman M.A., 1992, Regular and Chaotic Dynamics. Springer, Berlin
Lynden-Bell D., 1967, MNRAS, 136, 101
Mahon M.E., Abernathy R.A., Bradley B.O., Kandrup H.E., 1995, MNRAS, 275, 443
Matthews J, Walker R.L., 1964, Mathematical Methods of Physics. Benjamin, London
Merritt D., Valluri M., 1996, ApJ, 471, 82
Pettini M., 1993, Phys. Rev. E, 47, 828
Qian Q., Davidson R.C., Chen C., 1995, Phys. Rev. E, 51, R5216
Siopis C., Kandrup H.E., 2000, MNRAS, 319, 43
Strasburg S., Davidson R.C., 2000, Phys. Rev. E, 61, 5753
Van Kampen N.G., 1981, Stochastic Processes in Physics and Chemistry. North Holland, Amsterdam

This paper has been typeset from a TEX/LATEX file prepared by the author.